BRAIN COMMUNICATIONS

Altered neural oscillations underlying visuospatial processing in cerebral visual impairment

Alessandra Federici,[1,*] Christopher R. Bennett,[2,*] Corinna M. Bauer,[2] Claire E. Manley,[2] Emiliano Ricciardi,[1] Davide Bottari[1,†] and Lotfi B. Merabet[2,†]

* These authors contributed equally to this work.
† These authors contributed equally to this work.

Visuospatial processing deficits are commonly observed in individuals with cerebral visual impairment, even in cases where visual acuity and visual field functions are intact. Cerebral visual impairment is a brain-based visual disorder associated with the maldevelopment of central visual pathways and structures. However, the neurophysiological basis underlying higher-order perceptual impairments in this condition has not been clearly identified, which in turn poses limits on developing rehabilitative interventions. Using combined eye tracking and EEG recordings, we assessed the profile and performance of visual search on a naturalistic virtual reality-based task. Participants with cerebral visual impairment and controls with neurotypical development were instructed to search, locate and fixate on a specific target placed among surrounding distractors at two levels of task difficulty. We analysed evoked (phase-locked) and induced (non-phase-locked) components of broadband (4–55 Hz) neural oscillations to uncover the neurophysiological basis of visuospatial processing. We found that visual search performance in cerebral visual impairment was impaired compared to controls (as indexed by outcomes of success rate, reaction time and gaze error). Analysis of neural oscillations revealed markedly reduced early-onset evoked theta [4–6 Hz] activity (within 0.5 s) regardless of task difficulty. Moreover, while induced alpha activity increased with task difficulty in controls, this modulation was absent in the cerebral visual impairment group identifying a potential neural correlate related to deficits with visual search and distractor suppression. Finally, cerebral visual impairment participants also showed a sustained induced gamma response [30–45 Hz]. We conclude that impaired visual search performance in cerebral visual impairment is associated with substantial alterations across a wide range of neural oscillation frequencies. This includes both evoked and induced components suggesting the involvement of feedforward and feedback processing as well as local and distributed levels of neural processing.

1 IMT School for Advanced Studies, 55100 Lucca, Italy
2 The Laboratory for Visual Neuroplasticity, Department of Ophthalmology, Massachusetts Eye and Ear, Harvard Medical School, Boston, MA 02114, USA

Correspondence to: Lotfi B. Merabet, OD, PhD, MPH
Massachusetts Eye and Ear and Harvard Medical School
20 Staniford Street, Boston 02114, MA, USA
E-mail: lotfi_merabet@meei.harvard.edu

Correspondence may also be addressed to: Davide Bottari, PhD
IMT School for Advanced Studies Lucca
Piazza San Francesco 19, 55100 Lucca, Italy
E-mail: davide.bottari@imtlucca.it

Keywords: neural oscillations; cerebral visual impairment; feedforward; feedback; visual search

Received October 10, 2022. Revised June 16, 2023. Accepted August 25, 2023. Advance access publication August 28, 2023
Published by Oxford University Press on behalf of the Guarantors of Brain 2023.

Graphical Abstract

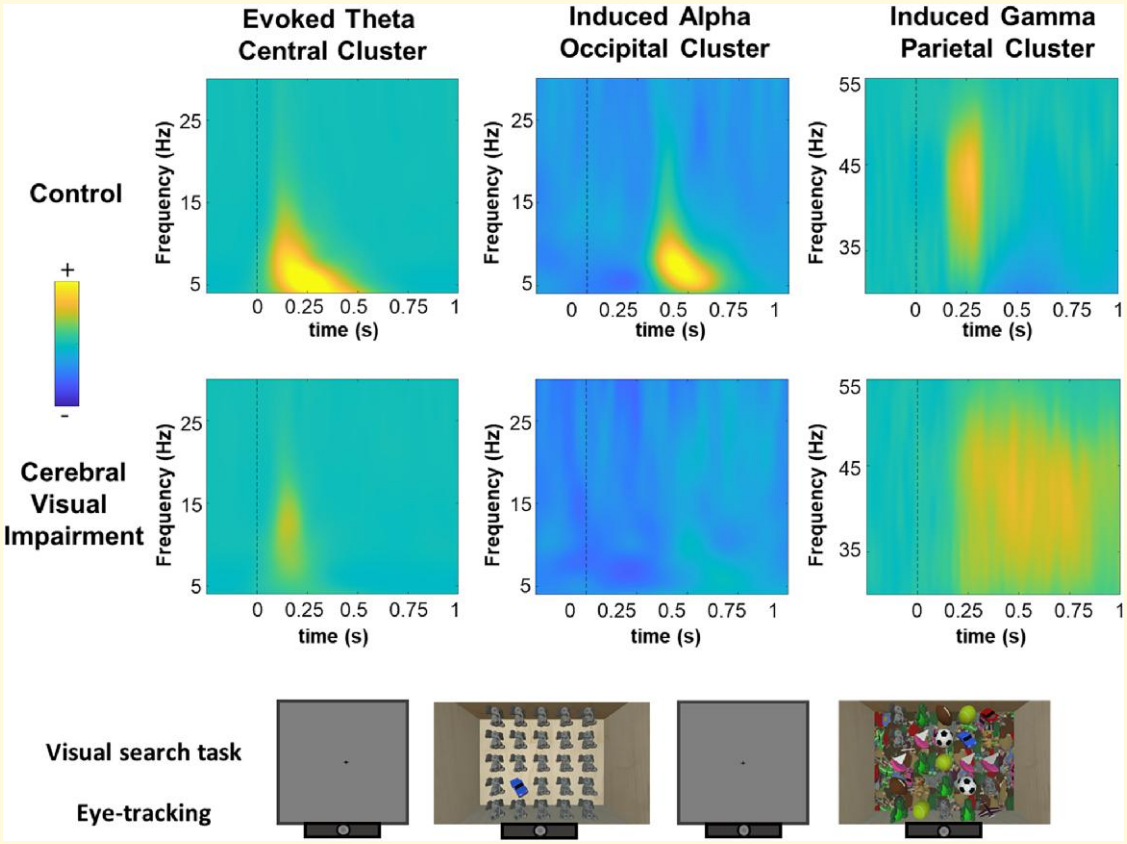

Introduction

Cerebral visual impairment (CVI) is a brain-based visual disorder associated with damage and/or maldevelopment of retrochiasmatic visual processing areas,[1,2] and is the leading individual cause of paediatric visual impairment in developed countries.[3-5] Early neurological damage (e.g. hypoxic-ischaemic injury, trauma, infection and genetic/metabolic disorders[6]) to visual pathways and higher-order processing areas of the brain are commonly very heterogeneous and thus contribute to the broad clinical presentation of visual impairments reported in this population.[7-10] Reduced visual acuity, visual field function, contrast sensitivity, as well as impaired ocular motor functions are all commonly observed in CVI. However, visual perceptual deficits related to higher-order visuospatial and visual attention processing are also highly prevalent,[4,7,8,11] even in cases where visual acuity and visual field functions are at normal or near-normal levels.[12,13] Interestingly, individuals with CVI often report difficulties interacting with complex and cluttered visual scenes.[9,14-16] For example, an individual may easily identify a favourite toy or recognize a familiar person when presented in isolation, yet have difficulties finding them in a cluttered toybox or in a crowd.[9,10,15] Taken together, these associated visual deficits can have a substantial impact on an individual's functioning, independence and well-being.[17] Despite representing a significant public health concern, the neurophysiological basis of CVI remains poorly understood. One important and unresolved question is as follows: are visuospatial processing deficits mainly driven by aberrant early stage sensory input, or are they the result of impaired higher-order visual processing mechanisms? Answering this question could be useful in identifying potential biomarkers of CVI, and potentially help inform the design of specific rehabilitative training strategies.

In clinical practice, visual-evoked potential (VEP) recordings have been used to assess the integrity of afferent visual pathways and lower-order functions (such as visual acuity), particularly in the case of infants and/or nonverbal patients who may not be able to undergo formal ophthalmic testing[3,18,19] (see Chang and Borchert[20] for review). Clinical VEPs are typically measured by averaging neural activity in response to passive viewing of simple visual stimuli such as flashes of light or patterns (e.g. gratings and chequerboards). The analysis of neural oscillatory activity may be more informative with respect to how information is encoded, transferred and integrated within the brain[21,22] from lower to higher processing stages. Two main categories of oscillatory responses, reflecting different aspects of neural activity, can be distinguished. Evoked neural oscillations are considered

to be precisely related to sensory input onset (phase-locked). In contrast, induced oscillations can be caused by external stimulation, but can also occur independently of it. They are not phase-locked to the onset of an external event, yet can reflect cognitive processes and the integration of sensory input and ongoing activity.[23-25] It has been suggested that these distinct components of neural oscillations are associated with different types of processing with respect to the direction of information flow.[25-28] Alterations in evoked activity could primarily reveal impairments with feedforward information processing along the thalamocortical pathway, while abnormal induced activity might be indicative of deficits in feedback processing associated with cortico-cortical connectivity (see Tallon-Baudry and Bertrand[25] and Yusuf *et al.*[29]). These distinct components of neural oscillations have been used to identify potentially important biomarkers of aberrant oscillatory activity in a variety of neurodevelopmental conditions including autism spectrum disorder,[30] dyslexia,[31] and other language-learning impairments.[32-34]

In a preliminary study, we recorded electroencephalography (EEG) signals while CVI participants carried out a virtual reality (VR)-based visual search task.[35] Using visual search as a proxy for visuospatial and visual attention processing abilities,[36] we found that impaired search performance in CVI was associated with a dramatic reduction in alpha desynchronization activity.[35] Given that alpha desynchronization is an important neural signal associated with visuospatial attention and distractor suppression,[37] these findings provided early evidence of altered neural processing in relation to higher-order visual perceptual deficits in this population. In the present study, we aimed to extend these findings by further investigating neural oscillatory activity in relation to manipulating visual search task difficulty as defined by the presence of clutter in a visual scene (i.e. complexity). By investigating a broad frequency range [4–55 Hz] of neural oscillations, as well as their evoked and induced related activities associated with overt visual search performance, we could better characterize the contribution of early stage and higher-order visual processing mechanisms in CVI. As a secondary aim, we also investigated putative associations between EEG activity and other clinical profile measures such as visual acuity as well as available structural morphometry data (MRI) in our CVI participants.

Materials and methods

Participants

A total of 26 individuals were recruited in this study. Ten participants were previously diagnosed with CVI (three females, mean age: 17.5 years old ± 2.59 SD) by experienced clinicians specializing in neuro-ophthalmic paediatric care (see Supplementary Materials '1. Diagnosis of CVI' for further details). All participants with CVI had visual impairments related to pre- or perinatal neurological injury and/or neurodevelopmental disorders. Causes of CVI included hypoxic-ischaemic injury related to prematurity including periventricular leucomalacia (PVL), hypoxic/ischaemic encephalopathy), seizure disorder, as well as genetic and metabolic disorders. Four out of the 10 CVI participants were born preterm (i.e. prior to 37 weeks gestation). Associated neurodevelopmental comorbidities included spastic and dystonic cerebral palsy. Best corrected visual acuities in the better-seeing eye ranged from 20/20 to 20/60 Snellen (0.0 to 0.5 LogMAR equivalent). CVI participants were also categorized according to previous functional criteria,[1] and the distribution of our study population was limited to categories 2 and 3 (definition of category 2: 40% defined as 'have functionally useful vision and cognitive challenges', and category 3: 60% defined as 'functionally useful vision and who can work at or near the expected academic level for their age group'). For a full list of CVI participant details, see Table 1. All CVI participants had a level of visual acuity, intact visual field function within the area corresponding to the visual stimulus presentation, as well as fixation and binocular ocular motor function sufficient for the purposes of completing the behavioural task requirements (including eye tracking calibration; see Supplementary Materials '2. Development of Visual Environment and Eye Calibration' for further details). Exclusion criteria included any evidence of oculomotor apraxia, intraocular pathology (other than mild optic atrophy), uncorrected strabismus, a visual field deficit corresponding to the area of testing, uncontrolled seizure activity, as well as cognitive deficits precluding the participant from understanding the requirements of the study.

Structural MRIs from CVI participants were assessed for brain lesion severity according to a reliable and validated semi-quantitative scale. The scoring procedure has been described in detail elsewhere.[38] Briefly, raw scores for each brain structure (e.g. lobe, subcortical structures, corpus callosum and cerebellum) were calculated and summed to provide a global (total of cortical and subcortical) lesion score, whereby a higher score is indicative of a greater degree of brain injury (representative images from CVI participants are shown in Supplementary Fig. 1).

Sixteen individuals with neurotypical development (five females, mean age: 19.2 years old ± 2.14 SD) were recruited as comparative controls. Control participants had normal or corrected to normal visual acuity and no previous history of any ophthalmic (e.g. strabismus and amblyopia) or neurodevelopmental (e.g. epilepsy and attention deficit disorder) conditions. The control and CVI groups were not statistically different with respect to mean age [$t(24) = 1.806$, $P = 0.084$].

Formal written consent was obtained from all the participants and a parent/legal guardian (in the case of a minor). The study was approved by the investigative review board of the Massachusetts Eye and Ear, Boston, MA, USA, and carried out in accordance with the Code of Ethics of the World Medical Association (Declaration of Helsinki) for experiments involving humans.

Table 1 CVI participant demographics

Subject ID	Sex	Age	Associated cause of CVI	Preterm/ term birth	CVI classification	Distance visual acuity OD—OS (Snellen)	Distance visual acuity OD—OS (LogMAR equivalent)	Global (total) lesion score (*n*/48)
1	Female	15	Birth complication, global developmental delay	Term	2	20/30–20/30	0.2–0.2	
2	Female	17	Meningitis, infarct	Term	3	20/50–20/60	0.4–0.5	8.5
3	Male	19	Decreased placental perfusion	Preterm	2	20/25–20/25	0.1–0.1	2.5
4	Female	21	Periventricular leucomalacia	Preterm	2	20/50–20/40	0.4–0.3	21
5	Male	19	Focal cortical atrophy, seizure disorder	Term	3	20/60–20/60	0.5–0.5	16
6	Male	15	Genetic	Term	3	20/20–20/20	0.0–0.0	4
7	Male	16	Infection	Term	2	20/25–20/25	0.1–0.1	11.5
8	Male	22	Periventricular leucomalacia	Preterm	3	20/40–20/25	0.3–0.1	26
9	Male	16	Unspecified, developmental delay	Term	3	20/20–20–20	0.0–0.0	2
10	Male	14	Periventricular leucomalacia	Preterm	3	20/25–20/25	0.1–0.1	16.5

Visual search task design and eye tracking

The behavioural task was a static object visual search based on a previously designed desktop VR-based naturalistic environment called the 'virtual toybox' (complete details regarding task design can be found in Bennett *et al.*[39], see also Manley *et al.*[40]). Briefly, the task represented a simulated rendering of a toybox viewed from an overhead, first-person perspective. Participants were instructed to search, locate and fixate a specific target toy (a blue truck) placed randomly among surrounding toys (and without overlap) serving as distractors in a 5×5 array. The target toy remained constant and was unique with respect to shape and colour so as to create a 'pop out' effect (akin to feature search). The arrays of toys were presented in a trial-by-trial fashion and pseudorandom order. Two levels of task difficulty ('low' and 'high') were used. In the low task condition, the target toy was surrounded by one unique distractor toy presented on a uniform background. In the high task condition, the target was placed alongside nine unique distractor toys and superimposed on a cluttered background scene designed to make target recognition more difficult (see Fig. 1). At a viewing distance of 60 cm, the virtual toybox subtended $\sim 38 \times 38°$ of visual angle. An equal number of low and high task conditions were presented. A trial consisted of viewing the toybox scene for 2 s followed by 1 s of a blank grey screen with a central fixation target. We did not incorporate an inter-stimulus jitter to maximize the possibility of predicting when the stimulus would have occurred. If one group (e.g. controls) was better at predicting stimulus onset, we would have a possible source of confound related to observed between-group differences. Trials were repeated 50 times per run, and 4 runs were collected (total of 200 trials). Each run lasted <2.5 min, with a brief rest period between each run.

Visual search performance outcomes and behavioural data analysis

Participants were seated comfortably in a quiet room, 60 cm in front of a 27″ LED monitor (ViewSonic 27″ Widescreen 1080p; 1920×1080 resolution). Visual search performance was quantified using three objective outcomes based on captured eye tracking data. Success rate measured the percentage of trials in which the participant found and fixated on the target in a given run. Successful fixation was defined as a sustained gaze that remained within the outer contour of the target for a minimum time of 400 ms. Reaction time corresponded to the time needed to find the target on the screen and was defined as the first moment the participant's gaze arrived within the outer contour of the target and remained fixated for at least 400 ms.[39,40] Gaze error was a continuous measure of a participant's ability to locate and accurately fixate the target.[39,40] This accuracy measure was defined as the distance between the centre of the target and the participant's gaze position and computed based on the sampling rate of the eye-tracker (90 Hz).

Statistical analyses of behavioural data were carried out using a mixed-model repeated measure ANOVA (with group as a between factor and condition as a within factor) and conducted separately for each of the visual search outcome measures. Since we investigated three behavioural measures, the correct adjusted *P*-value threshold was set to 0.017

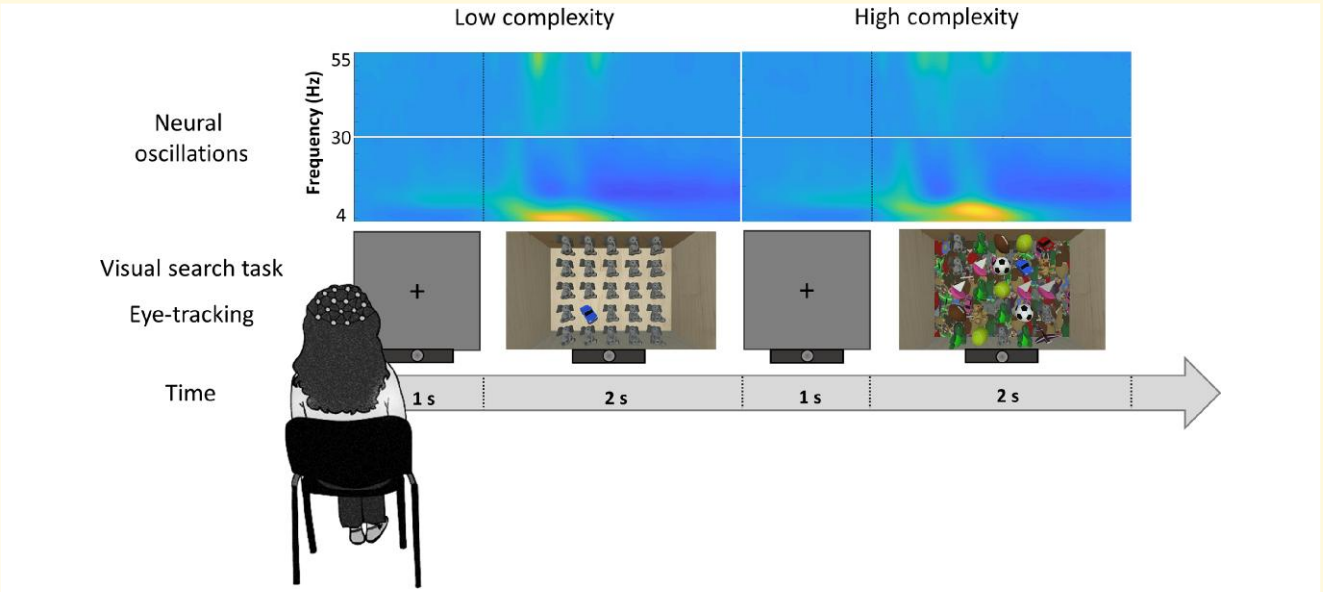

Figure 1 Experimental design. Illustrative figure showing a participant performing the visual search task while eye gaze patterns and EEG-related neural activity are recorded (putative neural oscillatory activity is shown in the *top* row). Two trials are shown, one for each visual task condition (low and high task difficulties).

(alpha level = 0.05/3). Analyses were performed using IBM SPSS v 26 Statistics Software.

Electrophysiological data acquisition, signal processing and analysis

Electrophysiological data were acquired while participants performed the visual search task using a wireless 20-channel Enobio system (Neuroelectrics, Barcelona, Spain; sampling rate of 500 Hz). This system was chosen for its simplified montage and setup procedure to minimize participant discomfort. After the recording cap was placed on the participant, conductive gel was added to each electrode site in order to enhance conductivity between the electrode and scalp surface. Once the montage was ready, signal quality was verified at each channel, and additional conductive gel was added if necessary to ensure adequate signal recording quality. Recording electrodes were made of a solid gel material and each channel was fed to a wireless (Bluetooth®) transmitter. Electrodes were arranged according to the standard 10–20 international system and covered the entire cap. An additional channel was inserted at the Oz position, given that we were primarily interested in measuring neural activity pertaining to visual processing. The reference channel was connected using a clip placed on the participant's right ear lobe. Signals were captured online and recorded by acquisition software running on a desktop computer located within 1 m of the participant.

EEG signal preprocessing was performed by implementing a validated pipeline to clean the data and promote reproducibility.[41,42] To improve independent component analysis (ICA) decomposition, each participant's continuous raw dataset was filtered (using a Hanning filter, low-pass cut-off at 40 Hz, filter order 50, and high-pass cut-off at 1 Hz, filter order 500[43]), downsampled at 250 Hz to reduce computational time and segmented in consecutive 1-s epochs, and epochs with a joint probability larger than 3 SD were excluded before computing the ICA.[44] An ICA based on the extended Infomax algorithm[45-47] was then performed, and the resulting weights were applied to the raw continuous unfiltered data.[41,42] Components associated with stereotypical eye blinks were identified and removed using a semi-automatic procedure (CORRMAP[48]). The template for blink components was chosen from the control group to ensure the selection of a typical artefact, and this template was used to find blink components across all participants (mean components removed for each individual in the CVI group = 0.9 ± 0.32 SD and control group = 0.94 ± 0.25 SD; see Supplementary Fig. 2 for the topography of each component removed in each participant). The number of rejected blink components was not statistically different between CVI and control participants ($P = 0.8$). All EEG activity associated with eye movements was retained due to the overt nature of the behavioural task and to avoid the risk of removing associated brain activity. Indeed, differences in eye movements could be due to altered brain activity, such as differences in the planning and execution of eye movements. Thus, eye movements cannot be considered artefacts in the present context.

Provided that ICA weights were applied to the raw continuous unfiltered data, preprocessing steps such as filtering, segmentation, noisy channel identification and interpolation, as well as noisy epochs rejection were carried out. Datasets were low-pass (60 Hz, filter order 26) and high-pass

(1 Hz, filter order 1000) filtered with a Hanning filter. Each continuous EEG signal was then segmented into epochs of 3 s (from −1 to 2 s with respect to the onset of the visual stimulus) and split between the low and high levels of task difficulty. Noisy channels were identified based on visual inspection and then interpolated using a spherical spline (mean interpolated electrodes per subject in the CVI group: 1.7 ± 1.06 SD and in the control group: 1.1 ± 0.84 SD). No statistically significant difference between the two groups emerged ($P = 0.1$). Following visual inspection, we rejected epochs exceeding a threshold of 150 μV within the [−0.5–1 s] time window representing contaminated portions of the EEG signal. The remaining epochs were further cleaned using a joint probability across channels with a threshold of ±3 SD .[44] In total, the mean retained epochs in the CVI group were 69.70 ± 10.56 SD for low and 72.10 ± 7.65 SD for high task difficulty trials. In the control group, this was 78.50 ± 10.46 SD for low and 77.94 ± 10.84 SD for the high task difficulty trials. An ANOVA investigating the number of retained epochs revealed no significant difference for the main effects of group and condition, nor a significant interaction between group and condition factors (all *P*-values > 0.08). Finally, we re-referenced the data to the average. An additional 40-Hz low-pass filter (order 50) was applied only before the computation of the event-related potential (ERP). All these steps were performed with EEGLAB software.[49] Data were then imported in Fieldtrip[50] to perform time-frequency decomposition, ERP and statistical analyses. We also extracted ERPs separately for the low and high levels of task difficulty for each group. Data were baseline-corrected, using a time window between −0.1 and 0 s before the visual stimulus presentation as the baseline.

The primary analysis of acquired EEG activity was focused on oscillatory activity associated with visual search behaviour. To this end, time-frequency decomposition of the EEG data was performed separately for the low and high levels of task difficulty within each group (CVI and controls). At the single participant level, we first extracted the induced power at each single trial after subtracting from each epoch the non-filtered ERP (i.e. computed for each participant without 40-Hz low-pass filtering) to remove the evoked activity from each trial. Single-trial time-frequency decomposition was computed at each electrode and separately for low [2–30 Hz] and high [30–55 Hz] frequency ranges. The higher frequency range was investigated up to 55 Hz to avoid line noise contamination (i.e. 60 Hz). Within the lower frequency range [2–30 Hz], oscillatory power was estimated using a Hanning taper with a frequency-dependent window length (4 cycles per time window) in steps of 2 Hz. Within the higher frequency range [30–55 Hz], oscillatory power was estimated using a Multitapers method with a Slepian sequence as tapers (in steps of 5 Hz) with a fixed-length time window of 0.2 s and fixed spectral smoothing of ±10 Hz. For both low and high frequency ranges, power was extracted over the entire epoch (from −1 to 2 s) and in steps of 0.02 s. Then, the average across trials was computed at the single-subject level for both conditions (i.e. low and high levels of task difficulty) and for the lower and higher frequency ranges. The resulting oscillatory activity was baseline-corrected to obtain the relative change with respect to the baseline period (for each frequency, the power at all time points was divided by the average power in the baseline interval). For the low frequency range, the baseline was set between −0.7 and −0.3 s, while for the high frequency range, this was set between −0.2 and −0.1 s. Lower frequencies (i.e. having a longer cycle) required a wider baseline window for appropriate estimation of slow oscillations and farther away from 0 to avoid temporal leakage of post-stimulus activity into the pre-stimulus baseline. The same procedure was implemented without ERP subtraction from single trials to estimate the total power from which the baseline-corrected evoked power was computed by subtracting the baseline-corrected induced power.

The same statistical approach was applied to all extracted electrophysiological measures. To investigate whether there was an interaction effect between the factors of group and task difficulty on oscillatory activities (i.e. evoked and induced components; low and high frequency ranges) and ERPs, we estimated the neural response change between conditions (differential activity computed from high minus low levels of task difficulty) within each group. Non-parametric cluster-based permutation (without *a priori* assumptions regarding sensors or time points) was performed between the CVI and control groups based on the difference between conditions (high-low). The Monte Carlo method with 1000 random permutations was applied and cluster-level statistics were calculated by taking the sum of the *t*-values within every cluster (minimum neighbour channel = 1; cluster alpha was set to 0.05 that was used for thresholding the sample-specific *t*-statistics). Identified clusters were considered significant for the permutation test at $P > 0.0125$ (the probability of falsely rejecting the null hypothesis). The alpha level of 0.05 was thus divided by 2 ($P = 0.025$) to account for the two EEG analyses (evoked and induced components of oscillations). Finally, this value was divided by 2 ($P = 0.0125$) to account for a two-sided test (positive and negative clusters). For ERPs, the cluster-based permutation analyses were performed across all electrodes and time points within the time window [0–0.5 s]. For time-frequency decomposition, statistical analyses were performed across all electrodes for time points within the time window [0–1 s] and across all frequencies within low [4–30 Hz] and high [30–55 Hz] ranges, and separately performed for induced and evoked oscillatory activities.

Note that the statistical time-frequency analyses were performed from 4 Hz (cycles of 250 ms) that is the first frequency at which the baseline could be estimated. If a significant interaction effect emerged, we assessed the difference between conditions within each group (i.e. low versus high task conditions in controls and low versus high conditions in the CVI group), and the difference between the two groups within each condition (i.e. controls versus CVI in the high task condition and controls versus CVI in the low task condition). In the absence of an interaction effect,

we collapsed the two conditions, performing the average between the low and high task difficulty conditions. These effects were all investigated with the same cluster-based permutation analysis approach and parameters described above ($P < 0.0125$).

Volumetric analysis of thalamic nuclei and pericalcarine cortex

Structural morphometry data were available from a subset of participants with CVI ($n = 9$). Of these, six were scanned using a T_1-weighted anatomical scan (TE 2.9 ms, TR 6.5 ms, flip angle 8°, isotropic 1-mm voxel size) acquired with a 32-channel phased array head coil (Philips 3T Elition X scanner). An additional three participants with CVI were scanned as part of a previous protocol (TE 3.1 ms, TR 6.8 ms, flip angle 9°, isotropic 1-mm voxel size) using an 8-channel phased array head coil (Philips 3T Intera Achieva). The volumes of predetermined thalamic nuclei [i.e. the lateral geniculate nucleus (LGN) and pulvinar] and the pericalcarine cortex were quantified for each subject in anatomical space using the FreeSurfer 7.2.0 (https://surfer.nmr.mgh.harvard.edu).[51-54] Segmentations for subcortical and cortical ROIs were derived from a probabilistic thalamic atlas[55] and the Desikan-Killiany atlas,[56] respectively.

Correlation analyses

We investigated putative associations between EEG activity and the clinical profile (i.e. age, visual acuity and global lesion classification) as well as available structural morphometry data (MRI) of our CVI participants using Spearman rank correlations followed by correction for multiple comparisons using False Discovery Rate (FDR).[57] Correlations between EEG activity and the volumes of the LGN, pulvinar and primary visual cortex were evaluated following adjustment for estimated total intracranial volume using residuals.

Results

Visual search task performance

We examined visual search performance on the effect of varying task difficulty with respect to all outcomes of interest. We conducted a series of mixed ANOVAs with group (CVI and control) as the between-subject factor and task difficulty (high and low) as the within-subject factor. In general, for all outcomes of interest (including success rate, reaction time and gaze error), we found a significant group difference between controls and CVI, with the CVI group having an overall impairment in visual search performance. A task difficulty difference between low and high conditions was found for reaction time and gaze error. No interaction effect between the task difficulty and group conditions emerged (see below).

CVI participants showed a lower mean success rate compared to controls. A mixed ANOVA revealed that the CVI group had a significantly lower success rate (low: 84.06% ± 21.18 SD, high: 81.30% ± 22.24 SD) than controls (low: 99.22% ± 2.15 SD, high: 98.28% ± 3.84 SD) [$F(1,24) = 9.141$, $P = 0.006$, $\eta p2 = 0.276$]. There was no effect of difficulty level [$F(1,24) = 2.36$, $P = 0.137$, $\eta p2 = 0.090$] and no interaction effect [$F(1,24) = 0.57$, $P = 0.458$, $\eta p2 = 0.023$] (Fig. 2A).

Mean reaction times were higher in the CVI group than controls. A mixed ANOVA showed that the CVI group had a significantly greater reaction time (low: 1447.39 ms ± 297.85 SD, high: 1519.07 ms ± 259.22 SD) compared to controls (low: 1035.38 ms ± 109.54 SD, high: 1122.30 ms ± 151.59 SD) [$F(1,24) = 29.27$, $P < 0.001$, $\eta p2 = 0.549$]. There was a significant effect of difficulty level [$F(1,24) = 6.69$, $P = 0.016$, $\eta p2 = 0.218$], but no interaction effect [$F(1,24) = 0.062$, $P = 0.806$, $\eta p2 = 0.003$] on reaction time. This suggests that the effect of task difficulty on reaction time was consistent across groups (Fig. 2B).

Mean gaze error (an index for visual search accuracy) was significantly higher in the CVI group. A mixed ANOVA showed that the CVI group had a significantly higher gaze error (low: 6.61 arc degrees ± 2.62 SD, high: 7.37 arc degrees ± 2.76 SD) than controls (low: 3.14 arc degrees ± 0.84 SD, high: 3.39 arc degrees ± 1.02 SD) [$F(1,24) = 27.275$, $P < 0.001$, $\eta p2 = 0.532$]. There was a significant effect of difficulty level [$F(1,24) = 11.985$, $P = 0.002$, $\eta p2 = 0.333$], but no interaction effect [$F(1,24) = 2.931$, $P = 0.100$, $\eta p2 = 0.109$]. This indicates that the effect of task difficulty on gaze error was consistent across groups (Fig. 2C, see also Supplementary Fig. 3 for representative examples of heat map displays of visual search patterns).

Examining putative associations between visual acuity in CVI participants (based on the LogMAR value of the better-seeing eye) and all visual search outcomes did not reveal any significant statistical correlations (all P-values > 0.24). Moreover, age did not emerge to be correlated with any behavioural measures of interest (all P-values > 0.53).

Finally, we assessed whether behavioural performance was associated with structural morphometry data (MRI). We observed a significant negative correlation between gaze error and the volume of the pulvinar nucleus ($r = -0.717$, $P = 0.03$). However, this did not survive FDR correlation for multiple comparisons ($P = 0.63$). There were no significant correlations between all the other behavioural outcomes and volume of the pulvinar, LGN and pericalcarine cortex, respectively (all P-values > 0.4).

Neural oscillations

Evoked power

Within the low frequency range [4–30 Hz], a cluster-based permutation test performed on the neural response change between the two levels of task difficulty and contrasting the control and CVI groups revealed an absence of a significant interaction (all P-values > 0.03). Thus, we collapsed the low and high levels of task difficulty, and a cluster-based permutation revealed a significant difference between the two

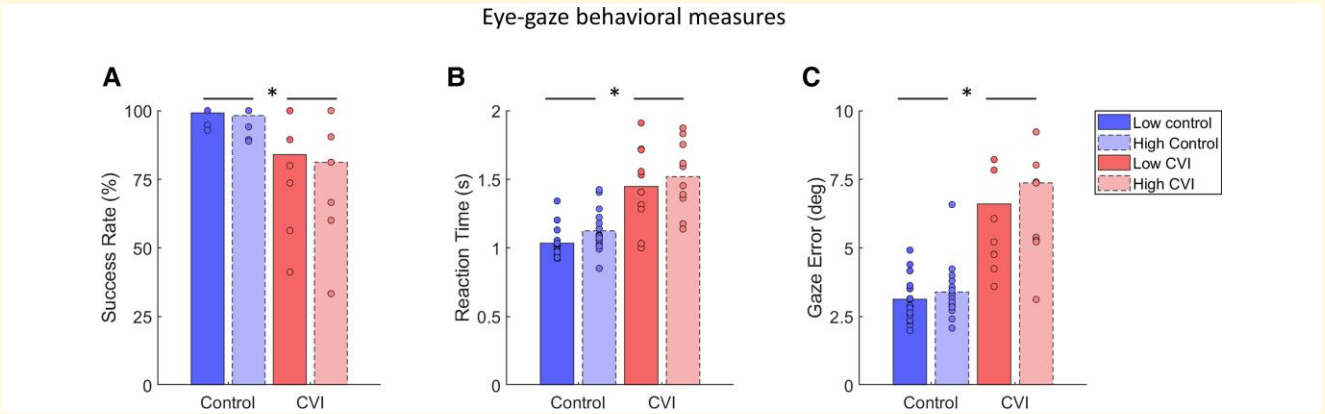

Figure 2 Behavioural outcomes. Group bar plots for the mean outcomes of visual search performance (**A**) success rate, (**B**) reaction time and (**C**) gaze error with respect to task difficulty (i.e. low and high). Each dot represents individual data. A mixed-model repeated measures ANOVA was conducted separately for each of the visual search outcome measures revealing that CVI participants showed an overall profile of impaired visual search compared to controls. Specifically, the CVI group had a significantly lower success rate ($P = 0.006$), greater reaction time ($P < 0.001$) and higher gaze error ($P < 0.001$). There was a significant effect of task difficulty level on reaction time ($P = 0.016$) and gaze error ($P = 0.002$) suggesting that the effect of task difficulty on reaction time and gaze error was consistent across groups (Fig. 2B and C).

groups ($P < 0.004$). In controls, visual stimulus presentation elicited strong theta activity [4–6 Hz] between 150 and 500 ms, starting at occipital regions and extending to central areas. This pattern was nearly absent in the CVI group (see Fig. 3A and B). No significant differences emerged at the high frequency range [30–55 Hz] (all *P*-values > 0.1; see Supplementary Fig. 4).

Induced power

Within the low frequency range [4–30 Hz], a cluster-based permutation test performed on the neural response change between task difficulty conditions and contrasting the control and CVI groups revealed a significant interaction between condition and group ($P < 0.005$). This interaction effect emerged within the alpha frequency band [8–14 Hz] at the occipital pole between 250 and 500 ms (see Fig. 4A and B). We explored this further by performing a cluster-based permutation analysis between the low and high task conditions within each group. In the control group, we found a significant modulation of alpha (and also extending into beta) band activity associated with task difficulty ($P < 0.001$). In contrast, no difference emerged in CVI participants (all *P*-values > 0.04). Moreover, when we investigated the difference between groups within each level of task difficulty, a cluster-based permutation analysis revealed a significant difference between the two groups for both low and high conditions (low: $P < 0.001$ and high: $P < 0.005$). In particular, the CVI group showed a reduction in alpha [10–16 Hz] desynchronization (>500 ms) within occipital channels in the low condition (this difference also extended into beta activity [12–22 Hz] at the high level of task difficulty; see Supplementary Fig. 5).

Within the high frequency range [30–55 Hz], a cluster-based permutation test performed on the neural response change between the two levels of task difficulty and contrasting the control and CVI groups revealed an absence of a significant interaction (all *P*-values > 0.04). Thus, we averaged the individual oscillatory responses across the low and high levels of task difficulty, and a cluster-based permutation analysis revealed a significant difference between the two groups ($P < 0.010$). The effect emerged between 300 and 700 ms in the occipital–parietal area. In the CVI group, sustained induced gamma [30–45 Hz] activity appeared to emerge compared to controls (see Fig. 5A and B).

Finally, to compare alterations in evoked and induced processing in CVI, we explored the relative strength of theta and alpha effects, respectively. We found that the effect size was very strong and comparable for both theta (Cohen's d = 1.55; CI: 0.66, 2.44) and alpha (Cohen's d = 1.45; CI: 0.57, 2.33).

ERP analysis

No significant differences emerged in the ERPs (all *P*-values > 0.034, see Supplementary Materials '3. Event Related Potential (ERP) Analysis' for details regarding the exploratory analysis and Fig. 6 for a visual representation of the results).

Associations between EEG activity and factors of interest in CVI participants

Relationship between EEG activity and volume of thalamic nuclei and primary visual cortex. There were no statistically significant correlations between the volumes of the LGN, pulvinar and pericalcarine cortex, and average theta, alpha or gamma activity nor P300 amplitude, respectively (all *P*-values > 0.4).

Relationship between EEG activity and age, visual acuity and global lesion classification. We did not observe any significant correlations between EEG activity (average theta, alpha or gamma activity nor P300 amplitude) and age (all

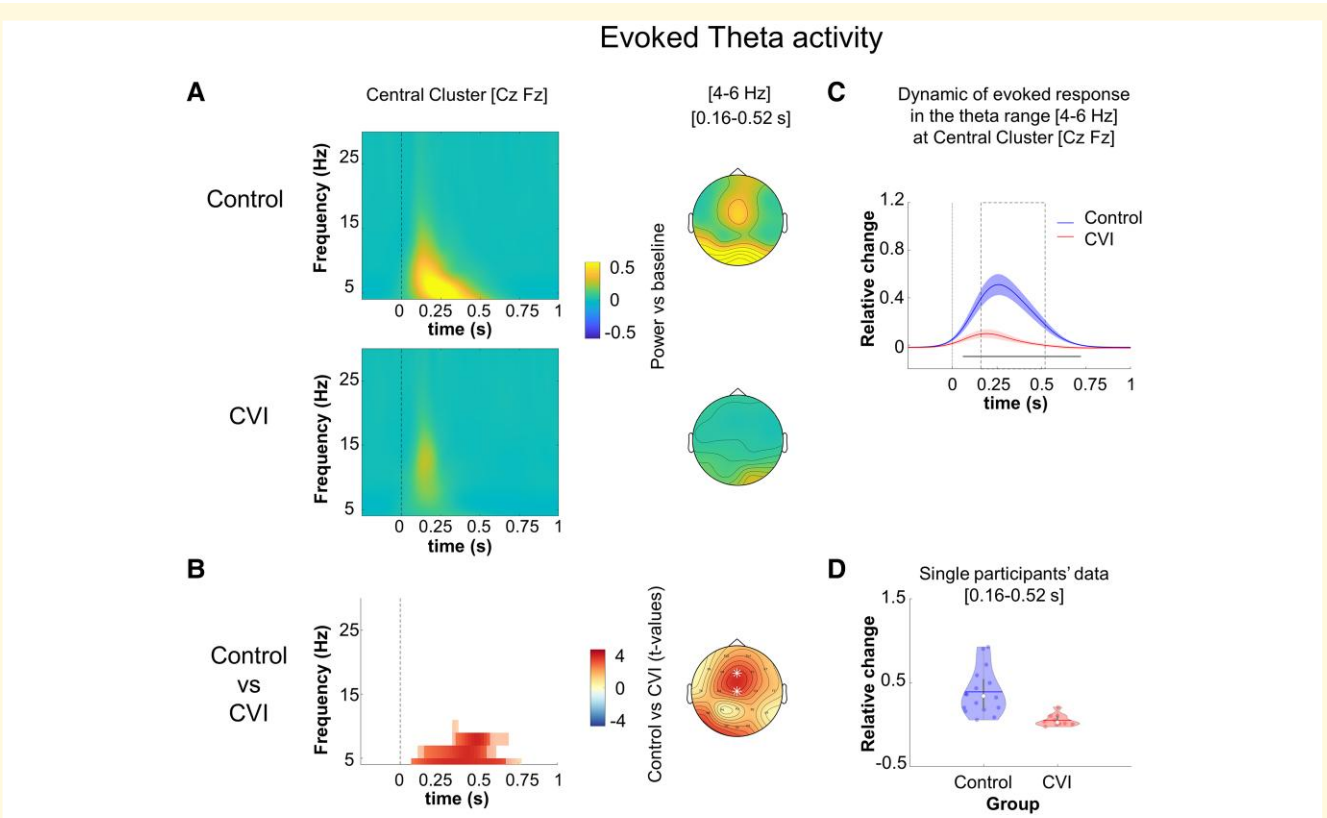

Figure 3 Evoked theta activity. (**A**) Oscillatory activity calculated as the average across low and high levels of task difficulty for controls (*upper* row) and CVI (*bottom* row) participants and plotted as a function of time [−0.25–1 s] and frequency [4–30 Hz]. The plots show the average between two representative central electrodes (Cz, Fz), and 0 s indicates stimulus onset. Scalp topographies in the theta range [4–6 Hz] within a representative time window [0.16–0.52 s] are shown (right panel). (**B**) Statistical results of the cluster-based permutation test. Time-frequency plot highlighting significant differences between control and CVI participants identified by the cluster-based permutation test ($P < 0.0125$) and corresponding topography for theta range [4–6 Hz] at a representative time window [0.16–0.52 s]. Electrodes belonging to the significant cluster are highlighted with white asterisks. (**C**) Time-course of the mean power in the theta range [4–6 Hz] for control and CVI subjects (data are averaged across two representative central electrodes Cz and Fz). Shaded areas represent SEM, and the continuous horizontal grey line indicates the significant difference between CVI and control groups (from 0.08 to 0.72 s; $P < 0.05$ FDR corrected). The dashed grey boxes represent the time window [0.16–0.52 s] comprising the theta peak in which theta power [4–6 Hz] was extracted for each subject (across channels Cz and Fz) and shown in the corresponding violin plots (**D**) with each dot representing individual data.

P-values > 0.1), LogMAR visual acuity (all *P*-values > 0.1) and extent of neurological damage (as defined by global lesion scores;[38] all *P*-values > 0.1).

Discussion

We analysed electrophysiological activity associated with higher-order visual perceptual impairments in individuals with CVI. At the behavioural level, CVI participants showed impaired visual search performance compared to controls as indexed by decreased success rate as well as increased reaction time and gaze error. This suggests that, in general, CVI participants were less likely, and took longer, in finding the target and that their search patterns were less accurate compared to controls. Importantly, behavioural performance in CVI did not correlate with visual acuity, suggesting that impaired visual search could not simply be explained by reduced stimulus visibility. This highlights the brain-based nature of higher-order visual perceptual deficits associated with this condition. In general, these observations appear in line with the clinical profile of CVI with respect to visuospatial and visual attention processing deficits reported in this population.[4,8]

The analysis of both evoked and induced oscillatory activities within a broad frequency range [4–55 Hz] revealed widespread alterations associated with impaired visual search in CVI participants compared to controls. Specifically, we found markedly reduced evoked theta [4–6 Hz] activity in the CVI group regardless of the level of task difficulty. Analysis of induced oscillatory activity revealed that the alpha signal was also markedly reduced in CVI compared to control participants. Furthermore, while induced alpha activity in controls was enhanced at higher task difficulty, this modulation was not evident in the CVI group. Moreover, the CVI group showed a greater sustained induced gamma response

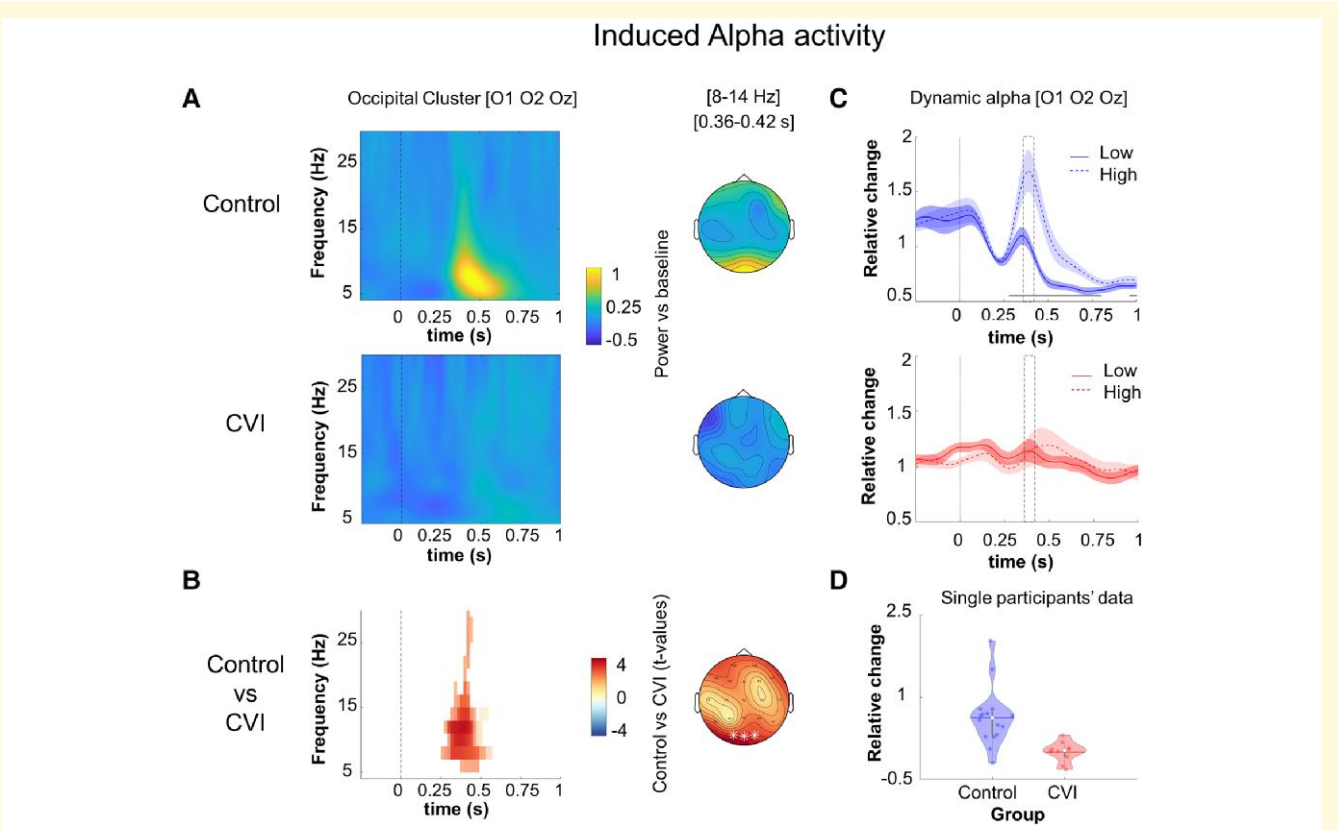

Figure 4 Induced alpha activity. (**A**) Oscillatory activity calculated as the difference between high and low levels of task difficulty is plotted for each group (controls: *upper* row and CVI: *bottom* row) as a function of time [−0.25–1 s] and frequency [4–30 Hz]. The plots show the average across three representative occipital electrodes (O1, O2, Oz), and 0 s indicates stimulus onset. Scalp topographies in the alpha range [8–14 Hz] at a representative time window [0.36–0.42 s] are shown (right panel). (**B**) Statistical results of the cluster-based permutation test. Time-frequency plot highlighting significant differences between control and CVI groups identified by the cluster-based permutation test ($P < 0.0125$) and the corresponding topography for the alpha range [8–14 Hz] at a representative time window [0.36–0.42 s]; electrodes belonging to the significant cluster are highlighted with white asterisks. (**C**) Time-course of the mean power in the alpha range [8–14 Hz] separately for the low and high levels of task difficulty is shown for the control and CVI groups (*upper* and *bottom* rows, respectively). Data are averaged across three representative central electrodes as follows: O1, O2 and Oz); shaded areas represent SEM; the continuous horizontal grey line indicates the significant difference between low and high levels of task difficulty in the control group (from 0.28 to 0.8 s; $P < 0.05$, FDR corrected). The dashed grey boxes represent the time window [0.36–0.42 s] comprising the alpha peak, in which the power in the alpha range [8–14 Hz] was extracted for each subject (across channels O1, O2 and Oz in both the high and low levels of task difficulty) and the difference high minus low task difficulty is shown in the corresponding violin plots (**D**), each dot represents individual data.

compared to controls. These alterations in both evoked and induced components of neural oscillatory activity suggest that impaired visual search in CVI is associated with anomalies in both feedforward and feedback signalling.

Phase-locked neural oscillations

The analysis of evoked oscillatory activity revealed a significant difference between CVI and control groups with respect to theta activity. In controls, a robust post-stimulus response in evoked theta [4–6 Hz] was found within the first 500 ms of visual stimulus presentation. However, in CVI, this theta activity was very much reduced independent of the level of task difficulty. Theta activity has been linked with the active sampling of input from the environment, with information processed at any given moment packed in each theta cycle.[58] Relevant to this study, successful visual search was found to be positively associated with post-stimulus theta amplitude in normally sighted individuals.[59] Interestingly, a subset of our study participants with CVI had visual acuities within normal/near-normal levels yet, impaired theta activity was still evident. This suggests that a reduction in evoked theta activity could be linked to a specific deficit in the organization of the neural responses phase-locked to visual events. In other words, even in the case of CVI participants having normal visual acuity, feedforward visual processing appears to be impaired in the setting of early neurological injury.

Non-phase-locked neural oscillations

Analysing induced oscillatory activity, we found evidence of two major alterations in the CVI group associated with alpha [8–14 Hz] and gamma [30–45 Hz] activity. In controls, occipital induced alpha activity increased with higher visual

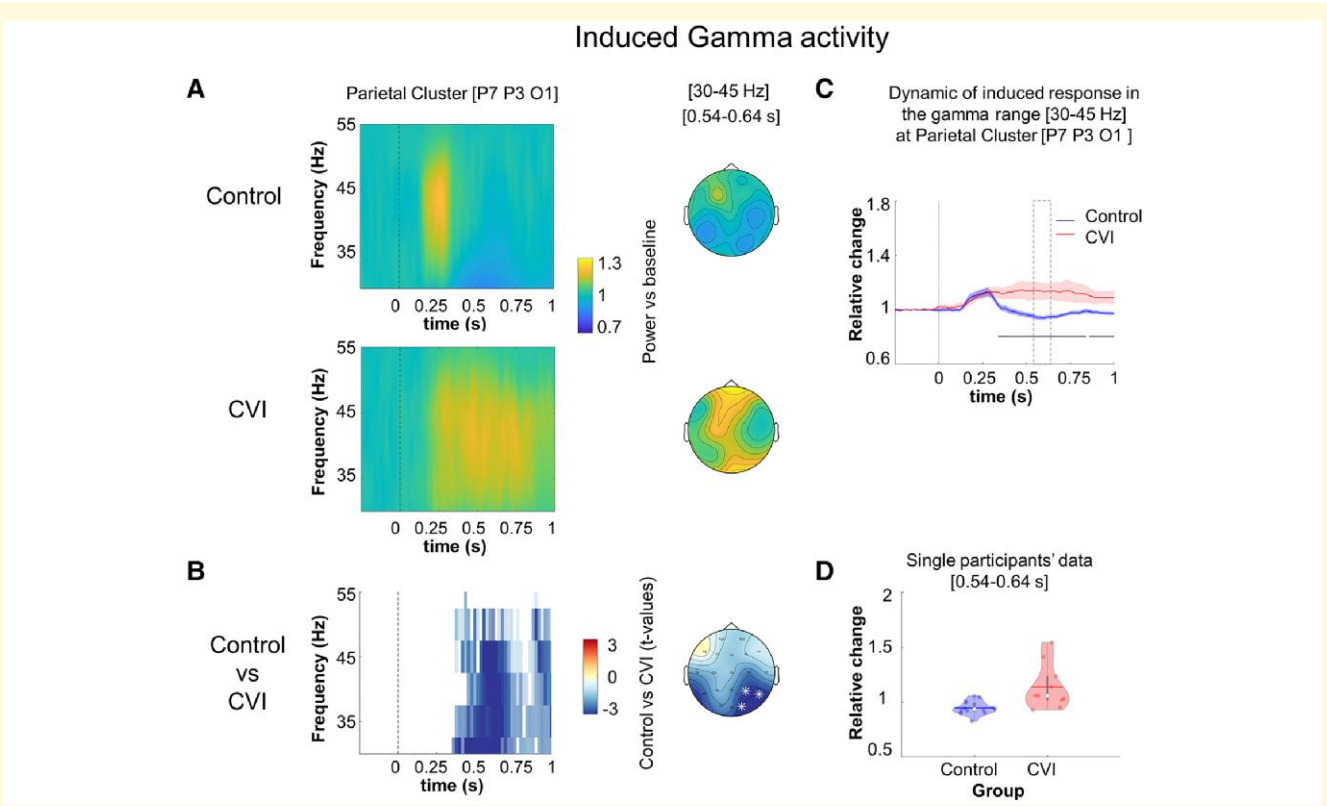

Figure 5 Induced gamma activity. (**A**) Oscillatory activity calculated as the average across low and high levels of task difficulty within each group (controls: *upper* row and CVI: *bottom* row) and plotted as a function of time [−0.25–1 s] and frequency [30–55 Hz]. The plots show activity at representative posterior electrodes (P7; P3; O1), and 0 s indicates stimulus onset. Scalp topographies in the gamma range [30–45 Hz] at a representative time window [0.54–0.64 s] are shown in the right panel. (**B**) Statistical results. Time-frequency plot highlighting significant differences between control and CVI groups identified by the cluster-based permutation test ($P < 0.0125$) and the corresponding topography for the gamma range [30–45 Hz] at a representative time window [0.54–0.64 s]. Significant electrodes belonging to the significant cluster are highlighted with white asterisks. (**C**) Time-course at the group level of the mean power in the gamma range [30–45 Hz] for control and CVI groups (data averaged across representative posterior electrodes P7, P3 and O1). Shaded areas represent SEM; continuous horizontal grey lines indicate significant differences between CVI and control groups (from 0.34 to 0.82 s and from 0.86 to 1 s; $P < 0.05$, FDR corrected). The dashed grey boxes represent the time window [0.54–0.64 s] in which the power in the gamma range [30–45 Hz] was extracted for each subject (in the electrodes P7, P3 and O1) and shown in the corresponding violin plots (**D**), each dot represents individual data.

task difficulty. However, this signal modulation was absent in CVI participants. Given the well-established link between alpha activity and visual attention,[37,60-62] this finding would be consistent with the view that neural mechanisms implicated with selecting visually attended targets and suppressing task-irrelevant stimuli are impaired in CVI.[63,64] A recent study by Gutteling *et al.*[65] reported that oscillations in the alpha band may be especially involved in distractor suppression and play a key role in closing the perceptual gate to distractor input. In the context of the results presented here, it is possible that CVI participants may have deficits with the inhibition of surrounding distracting information even in the case when viewing a visual scene with relatively low visual complexity.

In addition, CVI participants showed sustained induced gamma activity within posterior regions of the scalp and independent of the level of task difficulty. Gamma activity has been consistently associated with ocular movements such as micro-saccades.[66] Thus, it is possible that this aberrant pattern in gamma oscillatory activity in CVI could also be related to altered visual search behaviour. Consistent with this view, our visual search data suggest that gaze error (an index of gaze accuracy with respect to locating and accurately fixating the target) was significantly higher in CVI compared to control participants. The continuous need to recalibrate gaze while searching, locating and fixating on the target appears consistent with the pattern of sustained gamma band activity observed in CVI.

Neural markers of CVI and their potential clinical significance

To our knowledge, studies investigating electrophysiological activity (beyond VEP recordings) in relation to higher-order visual processing in CVI remain limited. A recent study by VerMaas *et al.* (2021) investigated children with CVI associated with cerebral palsy (CP) and used magnetoencephalography (MEG) to uncover oscillatory activity associated with

visuospatial processing abilities.[67] Consistent with the findings reported here, the authors found that participants with CP had weaker theta (as well as gamma) occipital activity related to impaired performance on their visuospatial processing and attention task. The authors proposed that these changes in oscillatory activity may be related to poor bottom-up processing of incoming visual information that in turn impacts higher-order visual processing and decision making.[67] This would be consistent with the alterations in evoked theta activity observed in our CVI participants. In our study, not all of our participants with CVI were diagnosed with CP nor had underlying neurological damage associated with PVL. Thus, our results further extend these observations to a broader profile of CVI as well as in relation to impaired visual search performance across multiple aetiologies associated with this condition. Moreover, widespread signal alterations in the CVI group were also evident regarding induced oscillatory activity, particularly with respect to the absence of alpha modulations.

Our findings appear to indicate that early-onset neurological damage impacts the correct development of both feedfoward and feedback processing. Normal development of feedforward connectivity is crucial for stimulus-driven sensory processing and seems to precede the elaboration of feedback connectivity, which in turn is important for top-down control of sensory processing and learning.[68,69] It has been suggested that early stimulus-driven learning plays a crucial role in elaborating feedback connectivity.[70,71] The present results might suggest that cortico-cortical feedback connectivity not only needs external visual input but also requires intact central processing to fully develop and operate. The relative combination of aberrant feedforward and feedback processing may represent a distinctive marker of CVI in relation to impaired visuospatial processing with respect to visual search abilities.

The identification of cerebral structures implicated with altered feedforward and feedback processing remains unclear but may be related to injury along thalamocortical visual pathways. In line with this view, we observed a significant negative correlation between gaze error and the volume of the pulvinar nucleus. This appears consistent given the important role this nucleus plays in the control of saccadic eye movements and the modulation of visual attention[72,73] (see also Strumpf *et al.*[74] for discussion of the pulvinar in distractor processing and visual search).

Study limitations and future considerations

Electrophysiological data in this study were recorded using a simple 20-channel EEG system to facilitate acquisition in the clinical setting and minimize participant discomfort (note that eye movements were also recorded with eye tracking). Given the reduced number of electrodes employed, we could not perform source modelling to localize neural sources of the electrophysiological activity. Future studies using our visual search paradigm combined with high-density EEG or MEG are therefore needed to further characterize the nature of the associated neural activity.

The relatively small sample size of our CVI group also represents an important limitation and is related to the challenges of subject recruitment for these types of studies. Specifically, due to the technical demands of this study, we recruited CVI participants within a limited range of visual functioning (i.e. visual acuity, visual field and contrast sensitivities, as well as ocular motor functions needed to maintain fixation) so as to minimize the effect of potential confounding factors that could influence visual search performance. Thus, this relatively narrow profile may limit the generalizability of our results to the overall CVI population. However, we also noted that the variance of data revealing theta and alpha effects (see Figs 3 and 4) was markedly higher in the control compared to CVI group. In particular, the SD for the evoked theta power within the 0.16–0.52-s time window was 0.27 and 0.07 for the control and CVI groups, respectively. Similarly, the SD for the induced alpha power within the 0.36–0.42-s time window was 0.53 and 0.19 for the control and CVI groups, respectively. Thus, the observed between-group neural differences cannot be merely ascribed to the heterogeneity of the CVI sample. Future studies using other behavioural assessment designs that can reveal a more robust profile relating performance and task difficulty in combination with EEG recordings could help to better characterize associations between impaired behavioural responses and oscillatory activity. Finally, we observed deficits in both feedforward (theta) and feedback (alpha) processing in the CVI group. However, data showed that their functional role was not the same. Only neural oscillations in the alpha range increased with task difficulty in controls. Importantly, this modulation was absent in CVI participants, indicating a specific role of this oscillatory activity in visual search behaviour and distraction suppression. Future studies may consider investigating relative contributions of feedforward and feedback activity in other visual contexts to understand their value as a potential biomarker and potentially help inform the design of specific training strategies.

In conclusion, results from this study suggest that participants with CVI have impaired visual search performance, consistent with previous accounts related to impaired visuospatial and visual attention processing. Impaired visual search performance was associated with marked alterations in neural oscillatory activity over a broad frequency range. This is consistent with widespread deficits within the visual system and implicates both local and distributed levels of neural processing. Finally, alterations of both evoked and induced components of oscillations suggest that both feedforward and feedback processing may be compromised in CVI.

Supplementary material

Supplementary material is available at *Brain Communications* online.

Acknowledgements

The authors would like to thank the subjects and their families for their participation in this study.

Funding

This work was supported by grants from the National Institutes of Health (NIH)/National Eye Institute (NEI) (R21 EY030587 and R01 EY030973) to L.B.M.

Competing interests

The authors report no competing interests.

Data availability

The data that support the findings of this study are available from the corresponding author, upon reasonable request and pending investigative review board approval.

References

1. Dutton GN, Lueck AH. Impairment of vision due to damage to the brain. In: Dutton AH, ed. *Vision and the brain: Understanding cerebral visual impairment in children*. AFB Press; 2015:3-20.
2. Sakki HEA, Dale NJ, Sargent J, Perez-Roche T, Bowman R. Is there consensus in defining childhood cerebral visual impairment? A systematic review of terminology and definitions. *Br J Ophthalmol*. 2018;102(4):424-432.
3. Good WV, Jan JE, Burden SK, Skoczenski A, Candy R. Recent advances in cortical visual impairment. *Dev Med Child Neurol*. 2001; 43(1):56-60.
4. Philip SS, Dutton GN. Identifying and characterising cerebral visual impairment in children: A review. *Clin Exp Optom*. 2014;97(3): 196-208.
5. Solebo AL, Teoh L, Rahi J. Epidemiology of blindness in children. *Arch Dis Child*. 2017;102(9):853-857.
6. Hoyt CS. Visual function in the brain-damaged child. *Review. Eye (Lond)*. 2003;17(3):369-384.
7. Boot FH, Pel JJM, van der Steen J, Evenhuis HM. Cerebral visual impairment: Which perceptive visual dysfunctions can be expected in children with brain damage? *A systematic review*. *Res Dev Disabil*. 2010;31(6):1149-1159.
8. Fazzi E, Signorini SG, Bova SM, *et al*. Spectrum of visual disorders in children with cerebral visual impairment. *J Child Neurol*. 2007; 22(3):294-301.
9. Lam FC, Lovett F, Dutton GN. Cerebral visual impairment in children: A longitudinal case study of functional outcomes beyond the visual acuities. *J Visual Impairment Blindness*. 2010;104(10): 625-635.
10. McKillop E, Dutton GN. Impairment of vision in children due to damage to the brain: A practical approach. *Br Ir Orthopt J*. 2008; 5:8-14.
11. Zihl J, Dutton GH. Chap 4 visual disorders. In: Zihl J, ed. *Cerebral visual impairment in children: Visuoperceptive and visuocogntive disorders*. Springer-Verlag; 2015:61-115.
12. van Genderen M, Dekker M, Pilon F, Bals I. Diagnosing cerebral visual impairment in children with good visual acuity. *Strabismus*. 2012;20(2):78-83.
13. Williams C, Northstone K, Sabates R, Feinstein L, Emond A, Dutton GN. Visual perceptual difficulties and under-achievement at school in a large community-based sample of children. *PLoS One*. 2011;6(3):e14772.
14. Dutton GN, Saaed A, Fahad B, *et al*. Association of binocular lower visual field impairment, impaired simultaneous perception, disordered visually guided motion and inaccurate saccades in children with cerebral visual dysfunction-a retrospective observational study. *Eye (Lond)*. 2004;18(1):27-34.
15. Jacobson L, Ek U, Fernell E, Flodmark O, Broberger U. Visual impairment in preterm children with periventricular leukomalacia—visual, cognitive and neuropaediatric characteristics related to cerebral imaging. *Dev Med Child Neurol*. 1996;38(8):724-735.
16. McDowell N, Dutton GN. Hemianopia and features of Balint syndrome following occipital lobe hemorrhage: Identification and patient understanding have aided functional improvement years after onset. *Case Rep Ophthalmol Med*. 2019;2019:3864572.
17. Chokron S, Kovarski K, Dutton GN. Cortical visual impairments and learning disabilities. *Front Hum Neurosci*. 2021;15:713316.
18. Skoczenski AM, Norcia AM. Development of VEP Vernier acuity and grating acuity in human infants. *Invest Ophthalmol Vis Sci*. 1999;40(10):2411-2417.
19. Watson T, Orel-Bixler D, Haegerstrom-Portnoy G. Early visual-evoked potential acuity and future behavioral acuity in cortical visual impairment. *Optom Vis Sci*. 2010;87(2):80-86.
20. Chang MY, Borchert MS. Advances in the evaluation and management of cortical/cerebral visual impairment in children. *Surv Ophthalmol*. 2020;65(6):708-724.
21. Buzsáki G, Draguhn A. Neuronal oscillations in cortical networks. *Science*. 2004;304(5679):1926-1929.
22. Siegel M, Donner TH, Engel AK. Spectral fingerprints of large-scale neuronal interactions. *Nat Rev Neurosci*. 2012;13(2):121-134.
23. Galambos R. A comparison of certain gamma band (40-Hz) brain rhythms in cat and man. In: Başar E and Bullock TH, eds. *Induced rhythms in the brain*. Birkhäuser; 1992:201-216.
24. Keil A, Bernat EM, Cohen MX, *et al*. Recommendations and publication guidelines for studies using frequency domain and time-frequency domain analyses of neural time series. *Psychophysiology*. 2022;59(5):e14052.
25. Tallon-Baudry C, Bertrand O. Oscillatory gamma activity in humans and its role in object representation. *Trends Cogn Sci*. 1999; 3(4):151-162.
26. Chen CC, Kiebel SJ, Kilner JM, *et al*. A dynamic causal model for evoked and induced responses. *Neuroimage*. 2012;59(1):340-348.
27. Lakatos P, O'Connell MN, Barczak A, Mills A, Javitt DC, Schroeder CE. The leading sense: Supramodal control of neurophysiological context by attention. *Neuron*. 2009;64(3):419-430.
28. Pfurtscheller G, Lopes da Silva FH. Event-related EEG/MEG synchronization and desynchronization: Basic principles. *Clin Neurophysiol*. 1999;110(11):1842-1857.
29. Yusuf PA, Hubka P, Tillein J, Kral A. Induced cortical responses require developmental sensory experience. *Brain*. 2017;140(12): 3153-3165.
30. Gandal MJ, Edgar JC, Ehrlichman RS, Mehta M, Roberts TP, Siegel SJ. Validating gamma oscillations and delayed auditory responses as translational biomarkers of autism. *Biol Psychiatry*. 2010;68(12): 1100-1106.
31. Goswami U. A temporal sampling framework for developmental dyslexia. *Trends Cogn Sci*. 2011;15(1):3-10.
32. Edgar JC, Khan SY, Blaskey L, *et al*. Neuromagnetic oscillations predict evoked-response latency delays and core language deficits in autism spectrum disorders. *J Autism Dev Disord*. 2015;45(2):395-405.
33. Heim S, Friedman JT, Keil A, Benasich AA. Reduced sensory oscillatory activity during rapid auditory processing as a correlate of language-learning impairment. *J Neurolinguistics*. 2011;24(5):539-555.
34. Murphy E, Benitez-Burraco A. Language deficits in schizophrenia and autism as related oscillatory connectomopathies: An evolutionary account. *Neurosci Biobehav Rev*. 2017;83:742-764.

35. Bennett CR, Bauer CM, Bex PJ, Bottari D, Merabet LB. Visual search performance in cerebral visual impairment is associated with altered alpha band oscillations. *Neuropsychologia*. 2021; 161:108011.
36. Treisman AM, Gelade G. A feature-integration theory of attention. *Cogn Psychol*. 1980;12(1):97-136.
37. Peylo C, Hilla Y, Sauseng P. Cause or consequence? Alpha oscillations in visuospatial attention. *Trends Neurosci*. 2021;44(9):705-713.
38. Fiori S, Cioni G, Klingels K, *et al*. Reliability of a novel, semi-quantitative scale for classification of structural brain magnetic resonance imaging in children with cerebral palsy. *Dev Med Child Neurol*. 2014;56(9):839-845.
39. Bennett CR, Bailin ES, Gottlieb TK, Bauer CM, Bex PJ, Merabet LB. Virtual reality based assessment of static object visual search in ocular compared to cerebral visual impairment. *HCI*. 2018;8:28-38.
40. Manley CE, Bennett CR, Merabet LB. Assessing higher-order visual processing in cerebral visual impairment using naturalistic virtual-reality-based visual search tasks. *Children (Basel)*. 2022; 9(8):1114.
41. Bottari D, Bednaya E, Dormal G, *et al*. EEG frequency-tagging demonstrates increased left hemispheric involvement and crossmodal plasticity for face processing in congenitally deaf signers. *Neuroimage*. 2020;223:117315.
42. Stropahl M, Bauer AR, Debener S, Bleichner MG. Source-modeling auditory processes of EEG data using EEGLAB and brainstorm. *Front Neurosci*. 2018;12:309.
43. Winkler I, Debener S, Muller KR, Tangermann M. On the influence of high-pass filtering on ICA-based artifact reduction in EEG-ERP. *Annu Int Conf IEEE Eng Med Biol Soc*. 2015;2015:4101-4105.
44. Delorme A, Sejnowski T, Makeig S. Enhanced detection of artifacts in EEG data using higher-order statistics and independent component analysis. *Neuroimage*. 2007;34(4):1443-1449.
45. Bell AJ, Sejnowski TJ. An information-maximization approach to blind separation and blind deconvolution. *Neural Comput*. 1995; 7(6):1129-1159.
46. Jung TP, Makeig S, Humphries C, *et al*. Removing electroencephalographic artifacts by blind source separation. *Psychophysiology*. 2000;37(2):163-178.
47. Jung TP, Makeig S, Westerfield M, Townsend J, Courchesne E, Sejnowski TJ. Removal of eye activity artifacts from visual event-related potentials in normal and clinical subjects. *Clin Neurophysiol*. 2000;111(10):1745-1758.
48. Campos Viola F, Thorne J, Edmonds B, Schneider T, Eichele T, Debener S. Semi-automatic identification of independent components representing EEG artifact. *Clin Neurophysiol*. 2009;120(5): 868-877.
49. Delorme A, Makeig S. EEGLAB: An open source toolbox for analysis of single-trial EEG dynamics including independent component analysis. *J Neurosci Methods*. 2004;134(1):9-21.
50. Oostenveld R, Fries P, Maris E, Schoffelen JM. Fieldtrip: Open source software for advanced analysis of MEG, EEG, and invasive electrophysiological data. *Comput Intell Neurosci*. 2011;2011:156869.
51. Dale AM, Fischl B, Sereno MI. Cortical surface-based analysis: I. Segmentation and surface reconstruction. *Neuroimage*. 1999; 9(2):179-194.
52. Fischl B, Salat DH, Busa E, *et al*. Whole brain segmentation: Automated labeling of neuroanatomical structures in the human brain. *Neuron*. 2002;33(3):341-355.
53. Fischl B, Sereno MI, Dale AM. Cortical surface-based analysis: II: Inflation, flattening, and a surface-based coordinate system. *Neuroimage*. 1999;9(2):195-207.
54. Fischl B, Van Der Kouwe A, Destrieux C, *et al*. Automatically parcellating the human cerebral cortex. *Cereb Cortex*. 2004;14(1): 11-22.
55. Iglesias JE, Insausti R, Lerma-Usabiaga G, *et al*. A probabilistic atlas of the human thalamic nuclei combining ex vivo MRI and histology. *Neuroimage*. 2018;183:314-326.
56. Desikan RS, Segonne F, Fischl B, *et al*. An automated labeling system for subdividing the human cerebral cortex on MRI scans into gyral based regions of interest. *Neuroimage*. 2006;31(3):968-980.
57. Benjamini Y, Hochberg Y. Controlling the false discovery rate: A practical and powerful approach to multiple testing. *J Royal Stat Soc*. 1995;57:189-300.
58. Colgin LL. Mechanisms and functions of theta rhythms. *Annu Rev Neurosci*. 2013;36:295-312.
59. Dugué L, Marque P, VanRullen R. Theta oscillations modulate attentional search performance periodically. *J Cogn Neurosci*. 2015; 27(5):945-958.
60. Bagherzadeh Y, Baldauf D, Pantazis D, Desimone R. Alpha synchrony and the neurofeedback control of spatial attention. *Neuron*. 2020;105(3):577-587 e5.
61. Clayton MS, Yeung N, Cohen Kadosh R. The many characters of visual alpha oscillations. *Eur J Neurosci*. 2018;48(7):2498-2508.
62. Romei V, Gross J, Thut G. On the role of prestimulus alpha rhythms over occipito-parietal areas in visual input regulation: Correlation or causation? *J Neurosci*. 2010;30(25):8692-8697.
63. Jensen O, Bonnefond M, VanRullen R. An oscillatory mechanism for prioritizing salient unattended stimuli. *Trends Cogn Sci*. 2012; 16(4):200-206.
64. Klimesch W. Alpha-band oscillations, attention, and controlled access to stored information. *Trends Cogn Sci*. 2012;16(12):606-617.
65. Gutteling TP, Sillekens L, Lavie N, Jensen O. Alpha oscillations reflect suppression of distractors with increased perceptual load. *Prog Neurobiol*. 2022;214:102285.
66. Yuval-Greenberg S, Tomer O, Keren AS, Nelken I, Deouell LY. Transient induced gamma-band response in EEG as a manifestation of miniature saccades. *Neuron*. 2008;58(3):429-441.
67. VerMaas JR, Lew BJ, Trevarrow MP, Wilson TW, Kurz MJ. Children with cerebral palsy have altered occipital cortical oscillations during a visuospatial attention task. *Cereb Cortex*. 2021; 31(7):3353-3362.
68. Dehaene-Lambertz G, Spelke ES. The infancy of the human brain. *Neuron*. 2015;88(1):93-109.
69. Kral A, Yusuf PA, Land R. Higher-order auditory areas in congenital deafness: Top-down interactions and corticocortical decoupling. *Hear Res*. 2017;343:50-63.
70. Batardiere A, Barone P, Knoblauch K, *et al*. Early specification of the hierarchical organization of visual cortical areas in the macaque monkey. *Cereb Cortex*. 2002;12(5):453-465.
71. Magrou L, Barone P, Markov NT, *et al*. How areal specification shapes the local and interareal circuits in a macaque model of congenital blindness. *Cereb Cortex*. 2018;28(8):3017-3034.
72. Dominguez-Vargas AU, Schneider L, Wilke M, Kagan I. Electrical microstimulation of the pulvinar biases saccade choices and reaction times in a time-dependent manner. *J Neurosci*. 2017;37(8): 2234-2257.
73. Saalmann YB, Pinsk MA, Wang L, Li X, Kastner S. The pulvinar regulates information transmission between cortical areas based on attention demands. *Science*. 2012;337(6095):753-756.
74. Strumpf H, Mangun GR, Boehler CN, *et al*. The role of the pulvinar in distractor processing and visual search. *Hum Brain Mapp*. 2013; 34(5):1115-1132.